

*Research Papers in Physics and Astronomy*

*Paul Burrow Publications*

---

University of Nebraska - Lincoln

Year 1995

---

Dissociative attachment in hot CH<sub>3</sub>Cl:  
Experiment and theory

D.M. Pearl\*  
Ilya I. Fabrikant<sup>‡</sup>

Paul Burrow<sup>†</sup>  
Gordon A. Gallup\*\*

\*University of Nebraska - Lincoln

<sup>†</sup>University of Nebraska - Lincoln, pburrow1@unl.edu

<sup>‡</sup>University of Nebraska - Lincoln, iif@unlserve.unl.edu

\*\*UNL, ggallup1@unl.edu

This paper is posted at DigitalCommons@University of Nebraska - Lincoln.

<http://digitalcommons.unl.edu/physicsburrow/11>

# Dissociative attachment in hot CH<sub>3</sub>Cl: Experiment and theory

D. M. Pearl, P. D. Burrow, I. I. Fabrikant, and G. A. Gallup

*Department of Physics and Astronomy, University of Nebraska, Lincoln, Nebraska 68588*

(Received 25 August 1994; accepted 9 November 1994)

The dissociative attachment (DA) cross section of hot CH<sub>3</sub>Cl has been measured in a crossed electron–molecule beam apparatus at temperatures up to 750 K and electron energies from 0–0.5 eV. The results are compared to cross sections computed using a mixed *ab initio*-semiempirical approach, treating CH<sub>3</sub>Cl as a quasidiatomic molecule. The theoretical treatment requires an anion potential curve in the stable region as a portion of the input data. Computations with three different basis sets show the results to be sensitive to the size of basis set from which the potential is determined. At high temperatures, the experimental DA cross sections are found to be in very good agreement with those derived from theory using the potential curve computed with the most flexible of the basis sets. At room temperature the theory suggests that the measured DA cross section is still limited by the presence of impurities. © 1995 American Institute of Physics.

## I. INTRODUCTION

As the prototype for monochloroalkanes, methyl chloride plays a special role in our understanding of the dissociative attachment (DA) process,



for these molecules in the gas phase. Unfortunately, because of its small size, the DA cross section of methyl chloride at room temperature and low electron energies is difficult to measure using either swarm or electron beam methods. Semiempirical calculations of Fabrikant<sup>1</sup> yield, near 0.6 eV, a peak in the DA cross section with a maximum of roughly  $10^{-23}$  cm<sup>2</sup> at room temperature. This is several orders of magnitude smaller than that found at 0.8 eV in a recent electron beam study by Pearl and Burrow.<sup>2</sup> This suggests that this experiment and others finding even larger cross sections are still limited by the presence of impurities. The theoretical results, however, have not yet been directly tested.

An alternate approach to the problem is to examine the temperature dependence of the DA process. From very general considerations, the cross section is expected to increase with temperature and shift to lower energies. At sufficiently high temperatures, the yield of Cl<sup>-</sup> from hot CH<sub>3</sub>Cl should overcome the signal contributed by the small amount of impurities present, affording an opportunity to compare experiment to theory. This implicitly assumes that the impurities must have large cross sections, i.e., their values are close to the theoretical maximum and do not increase substantially with temperature.<sup>3</sup>

The temperature dependence of the DA process in methyl chloride has been studied using swarm techniques by Datskos *et al.*,<sup>4</sup> who observed dramatic increases at electron energies near zero and 0.8 eV. Both of these features were confirmed in electron beam measurements of Pearl and Burrow.<sup>2</sup> However, it was found in the latter work that at elevated temperatures the upper peak, at 0.8 eV, arose from thermal decomposition of methyl chloride on the walls of the oven, producing HCl which has a large and distinctively shaped DA cross section peaking at this energy. In the

present paper, we will be concerned only with the lower peak which appears near zero energy.

The temporary negative ion states of CH<sub>3</sub>Cl, through which dissociative attachment should take place, have been studied both experimentally and theoretically. Electron transmission spectroscopy<sup>5</sup> (ETS) was employed by Burrow *et al.*<sup>6</sup> who located a broad resonance in the total scattering cross section centered at 3.45 eV. This feature was attributed to the temporary occupation of the C–Cl  $\sigma^*(8a_1)$  molecular orbital. The resonance energy and symmetry have been confirmed with stabilization calculations by Falcetta and Jordan<sup>7</sup> as well as multiple scattering  $X_\alpha$  calculations by Guerra *et al.*<sup>8</sup>

Further information about the temporary anion states has been derived from studies of the vibrational excitation of methyl chloride. A preliminary report by Shi *et al.*<sup>9</sup> confirmed the symmetry of the lower resonance by an examination of the vibrational modes which were excited and revealed the presence of a second resonance, of *e* symmetry, centered near 5 eV. Subsequently, measurements of the absolute vibrational excitation cross sections and the angular distributions of the scattered electrons have been carried out.<sup>10</sup>

A small DA cross section for methyl chloride is not difficult to rationalize since the vertical attachment energy lies above 3 eV and the lifetime of the resonance is correspondingly short. We note however that methyl chloride is quite different from the other monochloroalkanes in this regard. The DA cross section of ethyl chloride, for example, displays a peak in the yield of negative ions at 1.55 eV with a magnitude of  $1.49 \times 10^{-19}$  cm<sup>2</sup>, orders of magnitude larger than that of methyl chloride at room temperature. Other monochloroalkanes we have surveyed<sup>11</sup> also have similar or larger DA cross sections, peaked between 1.3–1.6 eV. The key difference appears to be the energies of the associated temporary anion states, which, in the latter compounds lie between 1.8 and 2.4 eV<sup>8</sup> as determined by ETS, well below that of methyl chloride.

To provide theoretical guidance for understanding the DA cross section of methyl chloride, Fabrikant<sup>1</sup> modeled this process using a semiempirical theory based on a combination

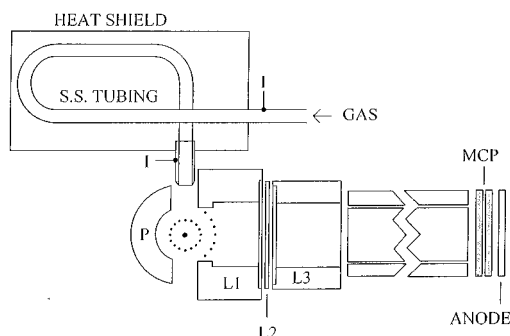


FIG. 1. Schematic diagram of the apparatus in a plane perpendicular to the electron beam. The heated gas line is rotated by  $90^\circ$  to appear in this plane for clarity.

of the resonance  $R$ -matrix approach and the non-local-complex-potential method. As noted earlier, it appears that the resulting cross section at room temperature is so small that it cannot be easily measured without extensive efforts to remove impurities. On the other hand, Fabrikant found that the cross section near zero energy increased rapidly with temperature and that above approximately 500 K, the yield of  $\text{Cl}^-$  from  $\text{CH}_3\text{Cl}$  should lie above the background due to impurities, assuming that the cross sections constituting the background do not change appreciably with temperature.

In the present work, we carry out a comparison of the experimental and theoretical DA data in methyl chloride at elevated temperatures and electron beam energies below 1 eV. We first review the means by which the measurements were carried out.

## II. EXPERIMENT

The apparatus is basically that discussed by Chu and Burrow<sup>12</sup> with a few changes as described in Pearl and Burrow.<sup>2</sup> Briefly, a magnetically collimated trochoidal monochromator<sup>13</sup> produces an electron beam that intersects, at right angles, the gas emerging from a heated gas tube. Figure 1 shows a cross section through the collision region in a plane perpendicular to the electron beam. A pusher electrode  $P$  directs ions produced along the electron beam through a series of electrodes L1, L2, and L3, and an 11 cm long cylinder whose purpose is to increase the distance between the microchannel plates used for ion counting and the heated gas line. The cylinder is divided into four quadrants, and an electric field is applied between two of the quadrants of the cylinder to offset the curvature of the ion trajectory caused by the magnetic field. The electron beam is partially shielded from the potential placed on the pusher electrode by a cylindrically positioned series of fine grid wires surrounding the beam.

The gas is heated by passing it through a length of resistively heated stainless-steel tubing. The gas line in the apparatus is actually in a plane parallel to the electron beam, but in Fig. 1 is shown rotated by  $90^\circ$  to appear in more detail. The tubing has an inner diameter of 1.9 mm and is shielded by a double layer of thin stainless-steel sheet. A length of

approximately 28 cm of the tubing is contained within the heat shield, and a chromel-constantan thermocouple placed roughly in the middle monitors the temperature. A short section of tubing at the gas exit end, approximately 2 cm long and shielded by a concentric metal tube, emerges from the heat shield and makes electrical contact with the wire carrying the heater current. A thermocouple also monitors the temperature at the exit of the tube. The conduction and radiation losses cause the temperature at this point to be lower than that in the main shielded section for temperatures above 300 K as discussed later.

An external valve enables the gas to be directed to the heated tubing or introduced into the background of the vacuum system. Contributions to the signal arising from the background gas are subtracted out. For this study, our source of  $\text{CH}_3\text{Cl}$  was the Aldrich Chemical Company, Inc. No further purification was carried out on the sample, which was described as better than 99.5% pure.

Energy scale calibration was carried out within  $\pm 0.1$  eV by reference to the peak<sup>14</sup> in the DA yield of  $\text{O}^-$  from  $\text{N}_2\text{O}$ . A more precise scale was obtained by use of the sharp peak near zero impact energy described more completely below.

The present apparatus is not well suited for measurements of absolute values of DA cross sections because of the uncertainties in the molecular beam density and profile as well as discrimination effects for fragment ions of kinetic energies above a few hundred meV. We have therefore referenced the ion currents measured at low electron energy to those coming from a peak appearing in the DA cross section at 7.4 eV. As noted elsewhere<sup>12</sup> this peak arises from predissociation of the lowest Feshbach resonance<sup>15</sup> in methyl chloride. Retarding potential measurements indicate that the ion fragment energies appear to be quite low and thus that kinetic energy discrimination problems should not be important. The magnitude of the 7.4 eV peak appears to be independent of temperature over the range of interest. This was verified in a mixture of methyl chloride and  $\text{N}_2\text{O}$  by reference to the 2.25 eV peak in the latter, which is known to be temperature independent.<sup>14</sup> The absolute DA cross section of the 7.4 eV peak,  $4.9 \pm 0.5 \times 10^{-20}$  cm<sup>2</sup>, was determined in a separate apparatus, described elsewhere,<sup>11</sup> consisting of a long static gas cell containing a total ion collection electrode.

## III. THEORY

### A. Scattering calculations

The details of the theoretical model are discussed elsewhere.<sup>1,16</sup> Basically,  $R$ -matrix theory is used to incorporate the resonant character of the scattering process and the long range (dipole and polarization) interaction between the incident electron and the molecule. The quasiclassical approach allows the efficient inclusion of the many vibrational channels that are necessary for a correct account of the survival probability of the intermediate negative ion. Our calculations have shown that if fewer than 35 vibrational channels are included, the DA cross sections exhibit qualitatively wrong behavior with regard to their energy dependence. The number of channels used in the present calculations was 50, which is enough for convergence.

TABLE I. The parameters for the  $R$ -matrix curves for each of the CH<sub>3</sub>Cl<sup>-</sup> potential curves.

Basis set	B	C	D	$\beta$	$\gamma_0$	$\gamma_1$	$\zeta$	$b$	$r_0$
A	0.166	0.029	-0.0097	0.7297	0.154	0.227	1.65	0.824	4.0
B	0.273	0.140	-0.0097	0.5256	0.16	0.22	1.65	0.824	5.0
C	0.170	0.038	-0.0097	0.5071	0.16	0.22	1.65	0.724	5.0

The theory was developed for diatomic molecules, and to apply it to methyl chloride we ignore all vibrations other than that corresponding to the C-Cl stretch and consider all other geometric parameters as functions of the distance  $R$  between the C and Cl atoms. The input data for the theory are the potential curves  $U_{\text{ion}}(R)$  and  $U_{\text{neut}}(R)$  for the negative molecular ion and the neutral molecule, respectively. These are described in detail below. In addition, the  $R$ -matrix parameter  $\gamma(R)$  describing the interaction between the resonant state and the continuum is required.

The form of the  $R$  matrix used is the same as that given before,<sup>1</sup>

$$\mathbb{R}(\rho) = \frac{\gamma^2(\rho)}{W(\rho) - E_e} + \mathbb{R}_b, \quad (1)$$

where  $\rho = R - R_e$ , the internuclear separation measured from the equilibrium distance,  $R_e$ ,  $\mathbb{R}_b$  is a background  $R$ -matrix term, and

$$W(\rho) = U'_{\text{ion}}(\rho) - U_{\text{neut}}(\rho). \quad (2)$$

In Eq. (2) the ion potential curve  $U'_{\text{ion}}$  is a modified form of the original adiabatic curve  $U_{\text{ion}}$  discussed above. The change is required to account for the specific long range potential and the different boundary conditions imposed on  $R$ -matrix wave functions from those on the wave functions of conventional variational structure calculations. The details of these considerations are discussed in Ref. 16.

In the initial theoretical study reported in Ref. 1, a negative-ion potential curve calculated by Falcetta and Jordan<sup>17</sup> was employed for  $R > R_{\text{cr}}$ , where  $R_{\text{cr}}$  is the internuclear distance at the crossing point between the neutral and negative ion potential curves. The experimental value of the vertical attachment energy was used to extrapolate  $U_{\text{ion}}(\rho)$  into the equilibrium distance  $R_e$ . However,  $\gamma$  remained uncertain, leading to variations of one or even two orders of magnitude in the DA cross section.

In the present calculations and those of Ref. 16, we have eliminated this uncertainty by using the experimental data of Shi *et al.*<sup>10</sup> for the vibrational excitation (VE) cross sections of CH<sub>3</sub>Cl. Electron excitation of the C-Cl stretch in the region between 1 and 5 eV is dominated by the  $a_1$  resonance.<sup>9</sup> The shape of the vibrational excitation cross section and its peak value are very sensitive to the vertical attachment energy and the  $\gamma$  parameter. This allows us to determine  $\gamma$  at the equilibrium internuclear distance with reasonable accuracy. Extrapolation to larger  $R$  can be performed using the electron affinity of the Cl atom, but the final results for the DA and VE cross sections are not sensitive to  $\gamma$  at large  $R$ .

As in Ref. 1, we used the following analytical forms

$$U'_{\text{ion}} = B e^{-2\beta\rho} - C e^{-\beta\rho} + D, \quad (3)$$

$$\gamma = \gamma_0 + \frac{\gamma_1}{e^{\zeta\rho} + b}.$$

We have performed these  $R$ -matrix calculations using the ion curves from three different basis sets, designated A, B, and C. These are described below, and Table I gives the results of our fitting procedure to determine the parameters of Eq. (3) for each of the curves, and also gives the value of  $r_0$ , the  $R$ -matrix sphere radius, used in each case. The value of the DA cross section has been found to be insensitive to reasonable changes in  $r_0$ . The parameters for the A basis set differ very little from those used in Ref. 1.

## B. Calculation of potential curves

The calculation of internuclear potential curves for negative ions presents formidable difficulties for theory. At separations greater than  $R_{\text{cr}}$ , the calculated energy of the ion is variationally stable. In such cases large flexible basis sets are required to obtain reasonable results. As one passes into the inner region,  $R < R_{\text{cr}}$ , the calculated energy of the ion using such a basis set will collapse, corresponding to a wave function that represents either a bound dipole state of the molecular anion<sup>18</sup> or one that represents an attempt of the basis set to imitate the neutral molecule and an electron in the continuum.<sup>19</sup> Which of these latter two alternatives occurs depends on the size of the basis set and whether the dipole moment of the neutral molecule is above the critical value. The anion state implicated in DA is, however, best represented by a configuration with the added electron in the normally unoccupied C-Cl  $\sigma^*$  antibonding orbital. In the outer region this configuration is the stable anion, but in the inner region it becomes a resonance, with a complex energy. The stabilization method<sup>20-22</sup> has been devised to obtain such complex energies using the basis sets of conventional bound state variational calculations, but we have not utilized this approach here.

Another difficulty arises in determining the potential curves that we have not addressed. In the discussion of the previous paragraph, the value of  $R_{\text{cr}}$  is not the actual crossing point, but depends upon the details of the basis set used and is the point where the *calculated* neutral molecule and anion curves cross. In practical calculations it will only approximate the true physical value. In particular, the anion curve will almost certainly be too high in energy relative to the neutral molecule curve because of deficiencies in treating electron correlation. We shall speak more of this below.

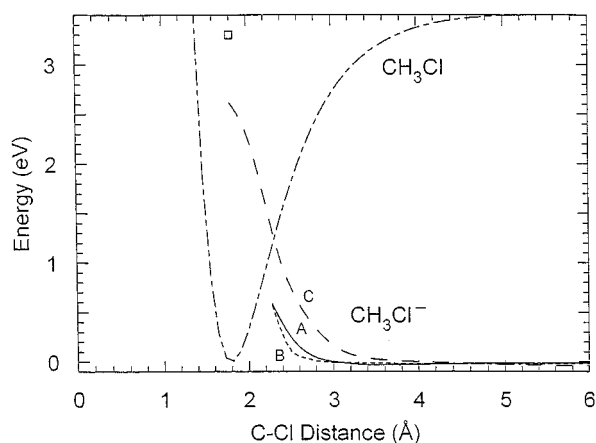


FIG. 2. Potential energy curves for the ground states of neutral CH<sub>3</sub>Cl and the <sup>2</sup>A<sub>1</sub> anion state as a function of the C–Cl distance. The basis sets are described in the text.—Basis set A, ---basis set B, and ----basis set C.---- gives the neutral molecule curve used. The point marked by □ is the experimental vertical attachment energy.

Theoretical studies of DA have emphasized the role of temporary negative ion formation as an essential part of the process.<sup>23–25</sup> A common practice in these studies is to use the Feshbach<sup>26</sup> projection operator formalism to force the wave function into representing the desired state. Although the projection is easily handled formally, in practice it constitutes a considerable restriction of the basis set used in contrast to the flexibility required for  $R > R_{cr}$ . There is, at present, no clear way to handle these conflicting requirements in calculating a negative ion potential curve at all distances. Furthermore, DA involves a mix of tunneling and activation processes and, therefore, has an exponential sensitivity to the physical parameters involved. These difficulties have required our mixing *ab initio* and semiempirical techniques in our calculations.

Accurate values of many parameters are required, such as the experimental electron affinity<sup>27</sup> (EA) of Cl and the experimental dissociation energy,<sup>28</sup>  $D_0(\text{C–Cl})$ , in methyl chloride. The calculated DA cross section is also sensitive to the precise values of the vibrational energies of the neutral molecule. Our procedure then, is to use the Morse function best reproducing the C–Cl stretching frequency of CH<sub>3</sub>Cl to represent it as a pseudodiatomic molecule for  $U_{\text{neut}}(\rho)$  and to use various calculated  $U_{\text{ion}}(\rho)$  curves, *shifted in energy to match the correct relative asymptotic energies determined from EA(Cl) and  $D_0(\text{C–Cl})$* .

Because of the theoretical uncertainties surrounding the negative ion potential curves, it is important to determine the sensitivity of the calculated DA cross sections to these input data. We have therefore used curves calculated with three different basis sets for comparison. These are shown in Fig. 2, together with the Morse function representation of the neutral molecule curve, described above. The open square in the figure marks the experimental vertical attachment energy.

*Set A.* Falchetta and Jordan<sup>17</sup> have computed the potential curve for  $R > R_{cr}$  using a large basis set, 6–311++G(2dp) at the UHF+MP2 level. The gap between curve A and the neu-

tral curve is due, at least in part, to the shift required to match the EA(Cl) and the  $D_0(\text{C–Cl})$ . It will be recalled from the discussion above that the variational collapse of the negative ion curve occurs at the crossing with the *computed* neutral molecule curve, rather than the crossing with the real experimental one.

*Set B.* We have employed a 6–31G basis with an extra set of *p* orbitals on Cl to help represent the Cl<sup>−</sup> ion and an off-center *s* function half-way between C and Cl to give polarization. This basis set was constructed as an attempted compromise between the conflicting flexibility requirements discussed above, but it is still too flexible to extend significantly into the inner region. The energies for this basis set were also determined at the UHF+MP2 level. The gap from the neutral curve in this case is caused by the same effects as for basis set A.

*Set C.* Finally, an unmodified 6–31G basis was tested with energies determined at the UHF level. With this basis set the ion curve can be extended considerably into the inner region as shown, but it gives, as we will see, a DA cross section that is much too small. Examination of Fig. 2 shows that the ion curve even with this basis set appears to be subject to some variational collapse at the smaller C–Cl distances. Falchetta and Jordan had already noted partial variational collapse with a 4–31G basis set.<sup>17</sup> Thus it is not surprising that the somewhat more diffuse 6–31G basis set also shows collapse.

In all these calculations the molecule was constrained to have  $C_{3v}$  symmetry, and the internal geometry of the methyl group was relaxed as a function of the C–Cl distance. Other geometries of CH<sub>3</sub>Cl<sup>−</sup> have lower energies,<sup>29</sup> but these are reached only for long C–Cl distances corresponding to essentially complete dissociation of CH<sub>3</sub>Cl<sup>−</sup>. They should, therefore, have an insignificant influence on DA, and we have ignored them.

As a peripheral comment, we note that the nature of basis set C that allows the ion curve to be carried so far into the inside region makes possible an interesting analysis of the problems using the Feshbach resonance theory. Selecting a particular finite basis set is equivalent to choosing a projection operator for a particular subspace of the total Hilbert space of the problem. Thus one might argue that the C ion curve represents the energy of the projected state of the Feshbach theory. Examination of Fig. 2 shows, however, that the experimental value of the vertical attachment energy is still considerably above this ion curve, which, in light of the Feshbach resonance theory, is unlikely. This may be seen because the position of the resonance from that theory is the solution of

$$E' = E_Q + \Delta(E'), \quad (4)$$

where  $E_Q$  is the energy of the projected state, and  $\Delta(E')$  is the integral

$$\Delta(E') = \frac{1}{2\pi} \int \frac{|\Gamma(E'')|^2 dE''}{E' - E''}, \quad (5)$$

which can be seen to be negative for  $E' = 0$ . Unless  $\Gamma$  has a very unusual energy dependence,  $\Delta(E')$  will be negative in a region above zero energy, and the actual position of the reso-

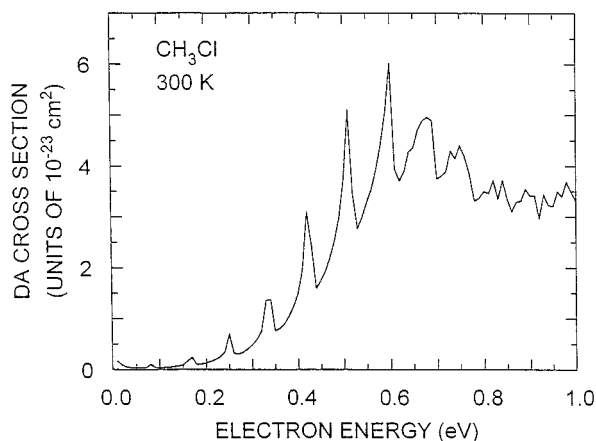


FIG. 3. The calculated dissociative attachment cross section of methyl chloride at 300 K as a function of electron energy. The negative ion potential curve of Falcetta and Jordan, Ref. 17, was used.

nance from the solution of Eq. (2) will be *below*  $E_Q$ . We conclude from this that even the relatively restricted 6–31G basis set is too unconstrained to serve effectively as a projection to obtain the energy  $E_Q$ , and that even the  $C$  ion curve indicates variational collapse into the continuum.

#### IV. RESULTS

Figures 3 and 4 show the calculated DA cross sections of methyl chloride at two representative temperatures, 300 and 600 K. Unless otherwise specified, all the calculated data incorporate the potential curve of Falcetta and Jordan.<sup>17</sup> The peak values of the cross sections vary by about three orders of magnitude over this temperature range. The sharp structures arise from the opening of successively higher vibrational channels of the neutral molecule and have been discussed previously.<sup>1</sup> For comparison with experiment, it is necessary to convolute the theoretical curves with the instrumental function. The latter was modeled with a Gaussian distribution whose full-width at half-maximum was chosen

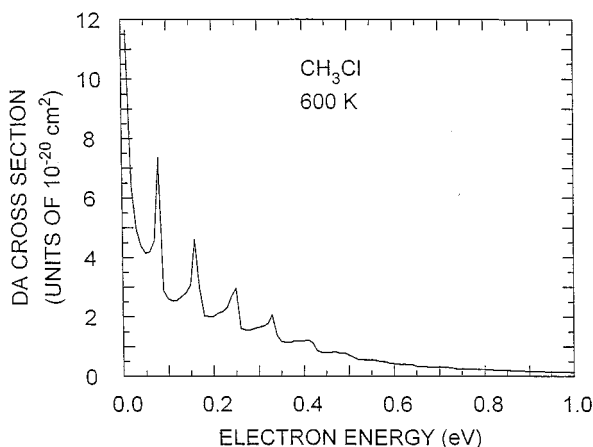


FIG. 4. The same as Fig. 3 at a temperature of 600 K.

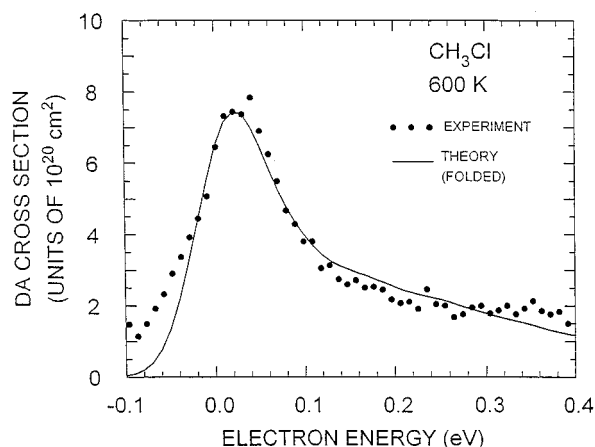


FIG. 5. The theoretical DA cross section at 600 K folded with a Gaussian distribution having a full-width at half-maximum of 67 meV. The experimental points are normalized to the theoretical curve at the peak.

to give best agreement between the folded theoretical curve and shape of the experimental peak. From measurements at three different temperatures, a full-width at half-maximum of 67 meV was chosen. Figure 5 illustrates the quality of the fit at 600 K. The magnitude of the experimental data is normalized to the theoretical curve and the energy scale shifted slightly, by about 40 meV, to agree. In our experience, the high energy wing of the electron distribution emerging from a trochoidal monochromator falls off slower than modeled by a Gaussian distribution, giving rise to the discrepancy at the lower energy end of the curve. Agreement over most of the curve is quite good. Unfortunately, the energy resolution is insufficient to observe the sharp threshold structures predicted by the unfolded theoretical data. At energies above about 0.3 eV, the experimental signal begins to increase due to contributions from HCl as discussed in detail elsewhere.<sup>2</sup> For completeness, we show in Fig. 6 the folded theoretical

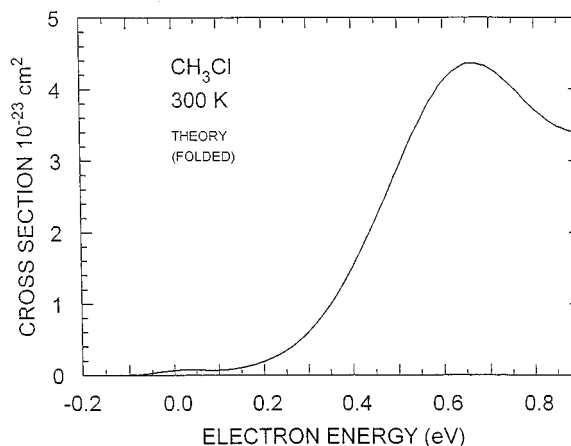


FIG. 6. The folded theoretical DA cross section at 300 K.

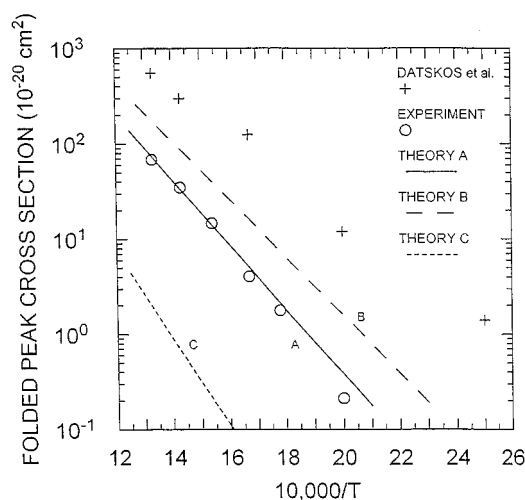


FIG. 7. The experimental and folded theoretical DA cross sections at their peaks plotted against inverse temperature. The open circles show the measurements from the present study. The solid and dashed lines show the computed results using the three negative ion potential curves. The + symbols indicate the peak cross sections unfolded from the swarm experiment of Datskos *et al.* (Ref. 4).

DA cross section at 300 K. The peak cross section at 0.66 eV is 43 times smaller than the experimental upper bound previously reported.<sup>2</sup>

Using the theoretical curves convoluted with the 67 meV Gaussian distribution, which was found above to give a reasonable representation of the instrumental function, we can now make a more direct comparison between theory and experiment as a function of temperature. At each temperature, the negative ion current was measured as a function of electron energy in the region below 1 eV and around the 7.4 eV peak. The maximum in the signal, which occurred close to zero energy, was placed on an absolute scale with an estimated error of  $\pm 25\%$  by reference to the cross section of the 7.4 eV peak. Theoretical cross sections were computed at six selected temperatures and convoluted with the Gaussian distribution.

In Fig. 7, the peak values of the experimental and folded theoretical cross sections are given on a semilog plot as a function of  $1/T$ . The solid line shows the theoretical dependence using the potential curve A. The agreement with the present data shown in open circles is exceptionally good and very likely fortuitous in part. The strong sensitivity of the calculated cross section to the location of the negative ion potential curve and its value at  $R_{cr}$  is shown by comparison with the dashed line, incorporating curve B, and the dotted line, using curve C.

In considering the results for the DA cross sections that arise from the three different determinations of the ion curves, it is clear that the two larger basis set MP2 calculations give much superior results compared with those of the minimal UHF calculation. Basis set A, the largest, gives results in best agreement with the experimental data, but basis set B is not far from this. From a variational point of view, the largest basis set A gives an overall 1.15 hartree (31.3 eV)

lower energy for the separated CH<sub>3</sub>+Cl<sup>-</sup> geometry, but the shift to the correct relative asymptotic energies hides this difference. Although the *shifted* set B curve falls slightly below the set A curve, we see that the original total electronic binding energies from the two calculations conform to our expectations that, variationally, the curve for set A should everywhere fall below that for set B. It is nevertheless gratifying that the sensitivity of the final DA cross sections to the details of the ion curve is no greater than this. The curve from set C, on the other hand, intersects the neutral curve at a much higher energy causing a substantial reduction in the DA cross section.

There is an additional experimental uncertainty regarding the temperature of the gas which should be pointed out. The data shown with open circles correspond to temperatures measured at the middle of the heated tube inside the heat-shielded region. As alluded to earlier, the gas line temperature declines over the last 2 cm of the heated tubing by an amount which is about 30% of the difference between the high temperature and 300 K. The effect of this decrease on the vibrational temperature of the emerging gas is difficult to estimate since the accommodation coefficients for the vibrational levels of methyl chloride on the surface are not known to us. It seems unlikely that the small number of wall collisions made in this short section of tubing are sufficient to substantially lower the vibrational temperature. However, as an example, if the temperatures were cooled to the average of the high temperature and that of the tube exit, the open circle data would shift to the right and fall approximately on the dashed line associated with potential curve B.

Figure 7 also includes the total electron attachment cross sections of Datskos *et al.*<sup>4</sup> derived from their swarm experiments. At the highest temperatures, their values lie about a factor of 10 higher than the folded theoretical cross sections, however, a direct comparison with the present work is not entirely justified. If their cross sections had been deconvoluted with infinite energy resolution, they should be tested against the *unfolded* theoretical cross sections. The low energy peak in their data, however, has a full-width at half-maximum of about 100 meV and peaks at approximately 30 meV. This appears to indicate an effective resolution at these low energies which may be comparable or somewhat larger than that used in the present experiment. In this case, we would conclude that the swarm data in fact lies consistently above the electron beam and theoretical results.

## V. SUMMARY

In this work we have shown that measurements of the dissociative attachment cross sections of hot CH<sub>3</sub>Cl at low electron energies are in remarkably good agreement with the predictions of a mixed *ab initio*—semiempirical theoretical treatment. The primary source of systematic error in the experimental results is likely to lie in our assumption that the vibrational temperature of the molecules is the same as the temperature measured at the hottest, longest, portion of the tube oven, and that there is negligible cooling at the exit end. If the effective gas temperature is lower than the measured value, our data points in Fig. 7 will be shifted to the right,

and for a given real temperature, the measured cross sections will lie above those predicted by the calculations we believe to be the most trustworthy.

The theoretical treatment, at this state in its development, is subject to a number of approximations. The strong dependence of the DA cross section on the location of the anion curve is amply illustrated, however, it is encouraging that large scale calculations of this curve are in good agreement with experiment. It remains to be seen whether calculations at this level will also be necessary in compounds like ethyl chloride that have much larger DA cross sections at room temperature.

The present theoretical approach still requires empirical data about the anion curve in the inner "resonance" region, namely, the vertical attachment energy and lifetime, which are obtained by fitting to the differential cross section for vibrational excitation. Both of these parameters are accessible in principle by theory, and our long term goal is to make the calculations fully *ab initio*. In addition, the approximation whereby CH<sub>3</sub>Cl is treated as a diatomic molecule needs to be removed by considering possible couplings with the *e* resonance and other vibrational modes.

Finally, we note that the predicted methyl chloride DA cross section at room temperature lies below that found in even the smallest reported beam measurement. This indicates that a more substantial effort to purify the compound and to remove impurities in the collision region will be required.

#### ACKNOWLEDGMENTS

This work was supported by the National Science Foundation through Grants No. CHE-8922601, CHE-9300941,

and PHY92-07386. We are pleased to acknowledge many useful conversations with Professor K. D. Jordan.

- <sup>1</sup>I. I. Fabrikant, *J. Phys. B*, **24**, 2213 (1991).
- <sup>2</sup>D. M. Pearl and P. D. Burrow, *Chem. Phys. Lett.* **206**, 483 (1993).
- <sup>3</sup>D. Spence and G. J. Schulz, *J. Chem. Phys.* **58**, 1800 (1973).
- <sup>4</sup>P. G. Datskos, L. G. Christophorou, and J. G. Carter, *Chem. Phys. Lett.* **168**, 324 (1990).
- <sup>5</sup>L. Sanche and G. J. Schulz, *Phys. Rev. A* **5**, 1672 (1972).
- <sup>6</sup>P. D. Burrow, A. Modelli, N. S. Chiu, and K. D. Jordan, *J. Chem. Phys.* **77**, 2699 (1982).
- <sup>7</sup>M. Falcetta and K. D. Jordan, *J. Phys. Chem.* **94**, 4037 (1992).
- <sup>8</sup>M. Guerra, D. Jones, G. Distefano, F. Scagnolari, and A. Modelli, *J. Chem. Phys.* **94**, 484 (1991).
- <sup>9</sup>X. Shi, T. M. Stephen, and P. D. Burrow, *J. Chem. Phys.* **96**, 4037 (1992).
- <sup>10</sup>X. Shi, V. K. Chan, and P. D. Burrow (in preparation).
- <sup>11</sup>D. M. Pearl and P. D. Burrow, *J. Chem. Phys.* **101**, 2940 (1994).
- <sup>12</sup>S. C. Chu and P. D. Burrow, *Chem. Phys. Lett.* **172**, 17 (1990).
- <sup>13</sup>A. Stamatovic and G. J. Schulz, *Rev. Sci. Instrum.* **41**, 423 (1970).
- <sup>14</sup>P. J. Chantry, *J. Chem. Phys.* **51**, 3369 (1969).
- <sup>15</sup>D. Spence, *J. Chem. Phys.* **66**, 669 (1977).
- <sup>16</sup>I. I. Fabrikant, *J. Phys B* **27**, 4325 (1994).
- <sup>17</sup>M. Falcetta and K. D. Jordan (unpublished).
- <sup>18</sup>K. D. Jordan, *Accts. Chem. Res.* **12**, 36 (1979).
- <sup>19</sup>T. Clark, *Faraday Discuss. Chem. Soc.* **78**, 203 (1984); *J. Chem. Soc., Chem. Commun.* **1984**, 93.
- <sup>20</sup>A. U. Hazi and H. S. Taylor, *Phys. Rev. A* **4**, 1109 (1970).
- <sup>21</sup>J. S.-Y. Chao, M. F. Falcetta, and K. D. Jordan, *J. Chem. Phys.* **93**, 1125 (1990).
- <sup>22</sup>B. Nestmann and S. Peyerimhoff, *J. Phys. B* **18**, 615, 4309 (1985).
- <sup>23</sup>J. N. Bardsley, A. Herzenberg, and F. Mandl, in *Atomic Collision Processes*, edited by M. R. C. McDowell (North-Holland, Amsterdam, 1964), p. 415.
- <sup>24</sup>T. F. O'Malley, *Phys. Rev.* **150**, 150 (1966).
- <sup>25</sup>W. Domcke, *Phys. Rep.* **208**, 97 (1991).
- <sup>26</sup>H. Feshbach, *Ann. Phys. (NY)* **5**, 357 (1958); **19**, 287 (1962).
- <sup>27</sup>H. Hotop and W. C. Lineberger, *J. Phys. Chem. Ref. Data* **14**, 731 (1985).
- <sup>28</sup>K. W. Egger and A. T. Cocks, *Helv. Chim. Acta* **56**, 1516 (1973).
- <sup>29</sup>T. Tada and R. Yoshimura, *J. Am. Chem. Soc.* **114**, 1593 (1992).